

Novel complex gratings with third-order group-delay variations for tunable pure dispersion slope compensation

Xuewen Shu, Elena Turitsyna, Kate Sugden, Ian Bennion

Photonics Research Group, Aston University, Birmingham, B4 7ET, United Kingdom
x.shu@aston.ac.uk

Abstract: We present a novel tunable dispersion compensator that can provide pure slope compensation. The approach uses two specially designed complex fiber Bragg gratings (FBGs) with reversely varied third-order group delay curves to generate the dispersion slope. The slope can be changed by adjusting the relative wavelength positions of the two FBGs. Several design examples of such complex gratings are presented and discussed. Experimentally, we achieve a dispersion slope tuning range of $\pm 650\text{ps/nm}^2$ with $>0.9\text{nm}$ usable bandwidth.

©2008 Optical Society of America

OCIS codes: (060.2340) Fiber optics components; (060.4510) Optical communications

References and links

1. Y. W. Song, Z. Pan, S. M. R. M. Nezam, C. Yu, Y. Wang, D. Starodubov, V. Grubsky, J. E. Rothenberg, J. Popelek, H. Li, Y. Li, R. Caldwell, R. Wilcox, and A. E. Willner, "Tunable dispersion slope compensation for 40-Gb/s WDM systems using broadband nonchannelized third-order chirped fiber Bragg gratings," *J. Lightwave Tech.* **20**, 2259 (2002).
2. W. H. Loh, F. Q. Zhou, and J. J. Pan, "Sampled fiber grating based-dispersion slope compensator," *IEEE Photon. Technol. Lett.* **11**, 1280 (1999).
3. C. K. Madsen, G. Lenz, A. J. Bruce, M. A. Cappuzzo, L. T. Gomez, and R. E. Scotti, "Integrated all-pass filters for tunable dispersion and dispersion slope compensation," *IEEE Photon. Technol. Lett.* **11**, 1623 (1999).
4. D. J. Moss, M. Lamont, S. McLaughlin, G. Randall, P. Colbourne, S. Kiran, and C. A. Hulse, "Tunable dispersion and dispersion slope compensators for 10Gb/s using all-pass multicavity etalons," *IEEE Photon. Technol. Lett.* **15**, 730 (2003).
5. X. Shu, I. Bennion, J. Mitchell, and K. Sugden, "Tailored Gires-Tournois etalons as tunable dispersion slope compensators," *Opt. Lett.* **29**, 1013 (2004).
6. C. S. Goh, S. Y. Set, K. Taira, S. K. Khijwania, and K. Kikuchi, "Nonlinearly strain-chirped fiber Bragg grating with an adjustable dispersion slope," *IEEE Photon. Technol. Lett.* **14**, 663 (2002).
7. J. Kwon and B. Lee, "Dispersion-order selectable chromatic dispersion compensator using strain-profile modification blocks," *IEEE Photon. Technol. Lett.* **15**, 1564 (2003).
8. S. K. Khijwania, C. S. Goh, S. Y. Set, and K. Kikuchi, "A novel tunable dispersion slope compensator based on nonlinearly thermally chirped fiber Bragg grating," *Opt. Commun.* **227**, 107 (2003).
9. S. Matsumoto, M. Takabayashi, K. Yoshiara, T. Sughara, T. Miyazaki, and F. Kubota, "Tunable dispersion slope compensator with a chirped fiber grating and a divided thin-film heater for 160 Gb/s RZ transmission," *IEEE Photon. Technol. Lett.* **16**, 1095 (2004).
10. P. I. Reyes, N. Litchinitser, M. Sumetsky, and P. S. Westbrook, "160-Gb/s tunable dispersion slope compensator using a chirped fiber Bragg grating and a quadratic heater," *IEEE Photon. Technol. Lett.* **17**, 831 (2005).
11. J. Kwon, S. Kim, S. Roh, and B. Lee, "Tunable Dispersion Slope Compensator Using a Chirped Fiber Bragg Grating Tuned by a Fan-Shaped Thin Metallic Heat Channel," *IEEE Photon. Technol. Lett.* **18**, 118 (2006).
12. M. Ibsen and R. Feded, "Fiber Bragg gratings for pure dispersion-slope compensation," *Opt. Lett.* **28**, 980 (2003).
13. J. Skaar, L. Wang, and T. Erdogan, "On the Synthesis of Fiber Bragg Gratings by Layer Peeling," *IEEE J. Quantum Electron.* **37**, 165 (2001).

1. Introduction

Chromatic dispersion and dispersion slope can cause adverse effects in optical communication systems, and both are especially problematic in high-speed transmission systems since the distortion of the optical signal resulting from chromatic dispersion/slope scales as the square of the signal bandwidth. Tunable dispersion compensators (TDCs) and tunable dispersion slope compensators (TDSCs) are crucial components in advanced high-speed systems, since the dispersion/slope compensation requirements can change due to the signal rerouting in reconfigurable network or even the variation of temperature and strain along fiber link which may degrade the system performance.

Dispersion slope problems may be divided into two cases: inter-channel slope and intra-channel slope. Inter-channel dispersion slope is where the different channels experience different amount of dispersion, this especially impacts on wavelength division multiplexing (WDM) systems and needs to be carefully considered when the bit rate is 10Gb/s or beyond. There are many schemes proposed to solve the inter-channel dispersion slope problem, such as multi-channel fiber Bragg gratings (FBGs) [1, 2], ring resonators [3], and Gires-Tournois etalons [4, 5]. Intra-channel dispersion slope is where the dispersion experienced by each wavelength component within an optical pulse is different, this distorts the signals within each channel. This problem has no significant influence in 10Gb/s system, but needs to be considered when the bit rate reaches 40Gb/s or beyond. To date, reported tunable intra-channel slope compensators are mostly based on FBG devices, such as dynamically applying nonlinear temperature, or nonlinear strain gradient, on a chirped FBG [6-11]. However, with these approaches the device itself can have a large chromatic dispersion and/or the dispersion varies simultaneously as the dispersion slope is tuned, so they are not pure TDSCs and contribute additional dispersion compensation [11,12]. In this paper, we present a pure TDSC based on twin novel nonlinear FBGs designed with layer-peeling inverse-scattering technique [13]. The distinct advantage of the proposed scheme here is that only the dispersion slope is tuned, and no additional dispersion is introduced. Also, the tuning mechanism is very simple (by adjusting the relative wavelength position of the twin FBGs) and no complex temperature or nonlinear strain gradient needs to be generated, therefore such a TDSC has very good reliability and stability.

2. Principle and design

The basic idea uses two complex FBGs with reversely varied third-order group delay curves to generate dispersion slope. The slope can be changed by adjusting the relative wavelength offset between the two FBGs. For such FBGs, the target spectra should have reflectivity that is square-like in profile and as close to 100% as possible, this minimizes the insertion loss and its variation when dispersion slope is adjusted. The bandwidth can be several nm according to applications. The dispersions for both gratings are quadratic functions, but reverse in shape, and can be described as:

$$D_1(\lambda) = 3A(\lambda - \lambda_0)^2 \quad (1)$$

$$D_2(\lambda) = -3A(\lambda - \lambda_0)^2 \quad (2)$$

where A is a constant.

If the wavelength of the FBG1 and FBG2 is shifted by $+\Delta\lambda$ and $-\Delta\lambda$, respectively, we can get the total dispersion

$$D_{total}(\lambda, \Delta\lambda) = D_1(\lambda + \Delta\lambda) + D_2(\lambda - \Delta\lambda) = 12A \cdot \Delta\lambda \cdot (\lambda - \lambda_0) \quad (3)$$

It is clearly seen from eqn.(3) that the dispersion is linearly varied along wavelength and its slope is derived as

$$DS(\lambda, \Delta\lambda) = 12A \cdot \Delta\lambda \quad (4)$$

It is noted from eqn (4) that the tuning range of dispersion slope is determined by the chosen constant A and the slope value is a linear function of the wavelength shift of two gratings.

The devices are designed by use of a layer-peeling inverse-scattering technique [13]. Figure 1 shows a design example for the case $A > 0$. The resulting real and imaginary part of the coupling coefficient along the grating length is shown in Fig. 1(a). The corresponding apodisation profile and period variation profile are shown in Fig. 1(b). It can be seen in Fig. 1(a) that the real and imaginary parts of the coupling coefficient have rapid oscillations near the grating centre. It is also seen in Fig. 1(b) that the grating apodisation has a sharp peak around the grating central position, which is also corresponding to a very fast period variation section.

Figure 1(c) shows the calculated reflection spectra with transfer matrix method by using the designed profile shown in Fig. 1(b). It can be seen in Fig. 1(c) that the group delay has third-order variation profile and the dispersion has quadratic variation profile.

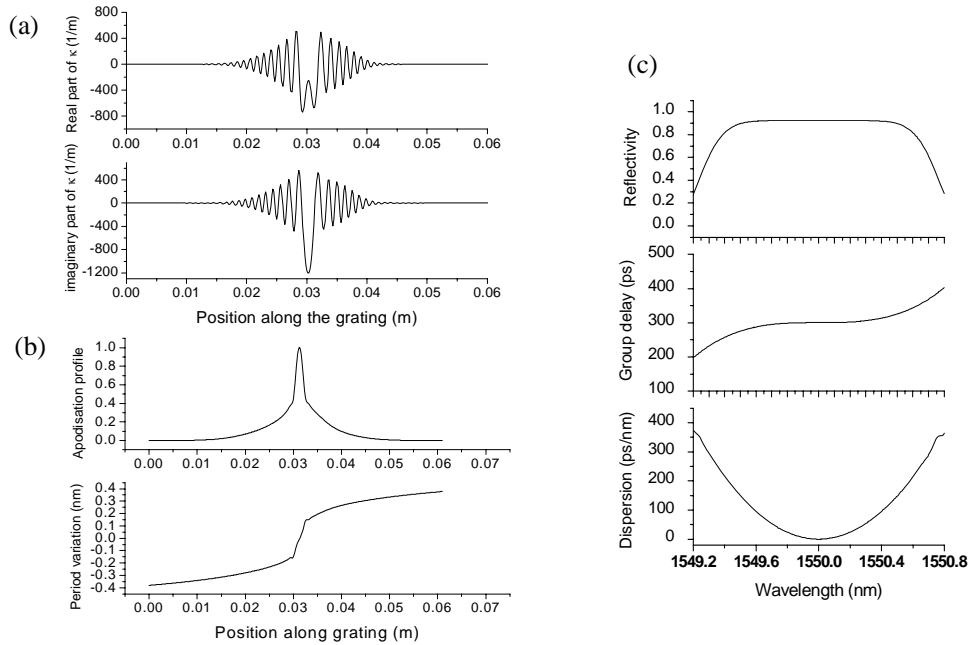


Fig. 1. Designed complex grating with $A > 0$. (a) Real and imaginary part of the coupling coefficient (κ). (b) Apodisation profile and period variation profile. (c) Calculated reflectivity, group delay and dispersion for the designed grating.

Similarly, one can design the corresponding grating with reversely varying group delay (the case $A < 0$). The resulting grating profile and simulated spectra are shown in Fig. 2. It is interesting to note that the real parts of the coupling coefficients of the two gratings are exactly the same, while the imaginary parts of the coupling coefficients of the two gratings have the same amplitudes but different signs. Comparing Figs. 1(b) and 2(b), we can also see that the apodisation profiles for the two gratings are very similar and the period variations for the two gratings are almost in reverse, which suggests that one can even possibly obtain the corresponding grating by simply changing the light launch direction of the original grating. This property can sometime simplify the device fabrication process.

Figure 3 shows the designs of such third-order gratings with different 3dB bandwidths. It can be seen from Fig. 3(a) that gratings with larger bandwidth have broader apodisation profiles, which indicate longer grating lengths are required. It is also seen from Fig. 3(b) that gratings with larger bandwidth have larger period variations.

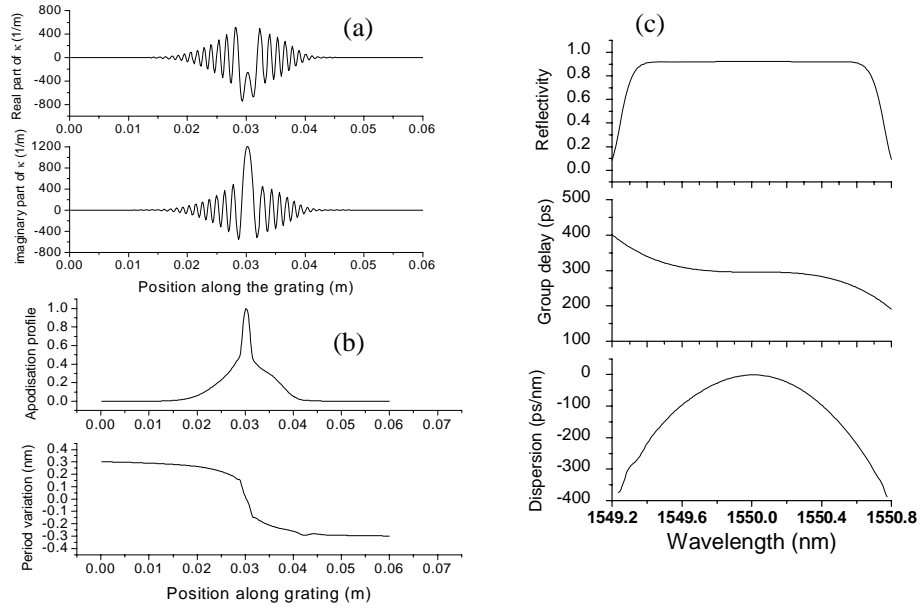


Fig. 2. Designed complex grating with $A < 0$. (a) Real and imaginary part of the coupling coefficient (κ). (b) Apodisation profile and period variation profile. (c) Calculated reflectivity, group delay and dispersion for the designed grating.

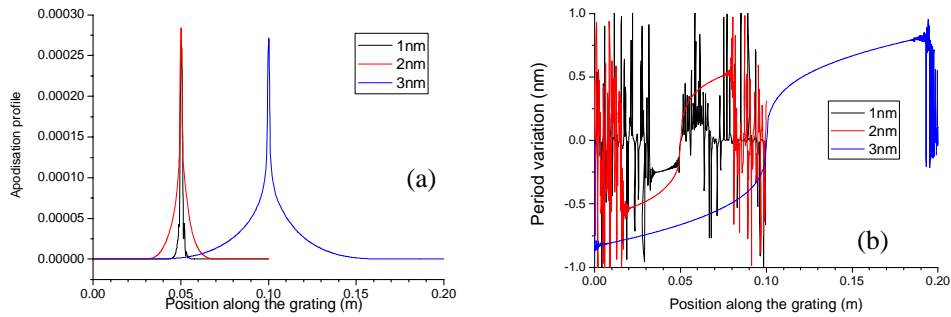


Fig. 3. Designed third-order group-delay gratings with different bandwidths. (a) Apodisation profiles; (b) Period variations.

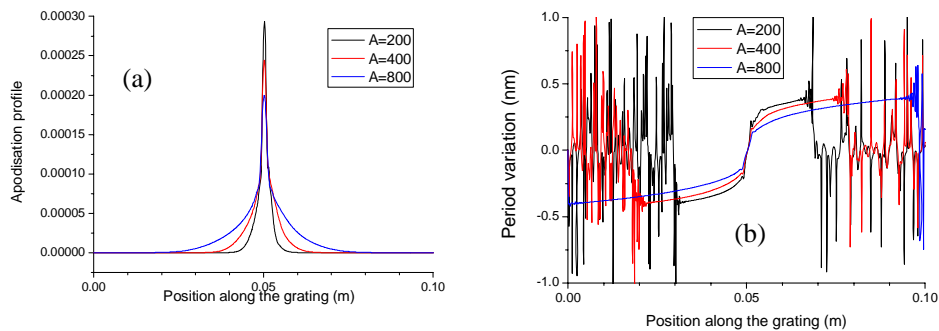


Fig. 4. Designed third-order group-delay gratings with different slope coefficients. (a) Apodisation profiles; (b) Period variations.

Figure 4 shows the designs of such third-order gratings with different slope coefficients (A). It is noted from Fig. 4(a) that gratings with larger slope coefficients have broader apodisation profiles, which indicate longer grating lengths are required. It is also noted from Fig. 4(b) that gratings with larger slope coefficients have smaller range of period variations. It should be pointed out that the sharp oscillation peaks in Fig. 3(b) and 4(b) are not important since they just appear near the grating edges and their corresponding index changes are close to zero (i.e. they can be truncated during fabrication).

3. Experimental results

We have fabricated the designed fibre Bragg gratings with a state of the art UV direct writing system developed at Aston University. The fabrication setup is schematically shown in Fig. 5(a), in which the UV writing beam ($\lambda=244\text{nm}$) was output from a frequency doubled argon ion laser and its beam size was reduced by a cylindrical focus lens. A small portion of uniform lithographic phase mask with a period of 1072.728 nm was used in the experiment. The fiber was mounted on an air-bearing translation stage moving at constant speed with good stability and accuracy, this approach allows the grating to be created pitch-by-pitch. The apodisation profile and the varied period were realized by appropriately controlling the ON/OFF of an AO-modulator and moving the phase mask/fibre. The structure was written in hydrogen loaded optical fibre. The fabricated devices were characterized with the Agilent Chromatics Dispersion Test Set (86073C). The wavelength resolution and the modulation frequency were set at 2.5pm and 250MHz, respectively.

Figure 5(b) shows the measured reflectivity and group delay response of one of the FBGs. As expected, the group delay varies as a third order function. It is interesting to note that if one reverses the light launch direction, the reversely varied third order group delay can be generated, as shown in Fig. 5(c). Figure 5(d) show the dispersion spectra for the both light launch directions. The dispersion has been averaged using a 0.2nm window when calculated from the measured group delay data. It is seen clearly in Fig. 5(d) that the dispersion curve are quadratic for both light launch ends.

The tunable dispersion slope compensator was built using two such gratings and a 4-port optical circulator (see the inset in Fig. 6(a)). The wavelength of the gratings was shifted by applying uniform strain along the optical fiber and no additional group delay/dispersion ripples were expected to be introduced by this simple method. Figure 6 shows the measured group delay response and the insertion loss of the tunable dispersion slope compensator when the dispersion slope was set at different values. It is seen that the dispersion slope can be tuned continuously from $-650\text{ps}/\text{nm}^2$ to $+650\text{ps}/\text{nm}^2$. The slope can be adjusted further, but at the expense of the bandwidth of the device, which can be seen in Fig. 6(b). The 3dB bandwidth of the TDSC is about 0.9nm for the setting of $\pm 650\text{ps}/\text{nm}^2$. The insertion loss is about 4dB (including about 2.5dB loss from the optical circulator) and the insertion loss variation is about 0.5dB for the full tuning range. The variation of the insertion loss is due to variations on the reflectivity of one of the gratings, and can be improved if both the gratings have better reflectivity flatness. Figure 6(c) shows the dispersion curves of the TDSC, which have relatively good linearity (with a 0.3nm average window). The group delay ripples (GDR) of the TDSC are plotted in Fig. 6(d), which are the deviations from the best fit quadratic curve and are averaged over 0.1nm. It is seen that the GDR for all the slope settings are relatively small ($\pm 4\text{ps}$).

4. Conclusions

We have designed and fabricated novel gratings with reversely varied third-order group delay curves. Such gratings can be combined to provide tunable pure dispersion slope compensation. Such gratings will find applications in high-speed optical transmission systems.

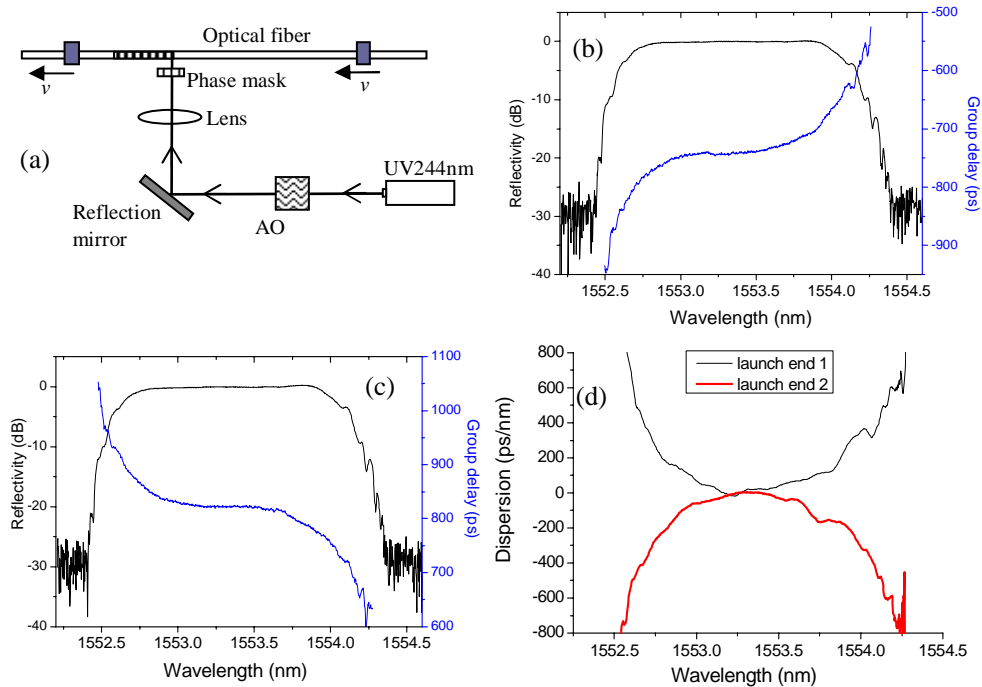


Fig. 5. (a) Schematic of the fabrication setup. (b) and (c) Measured reflectivity and group delay of a FBG sample with different light launch sides. (d) Corresponding dispersion.

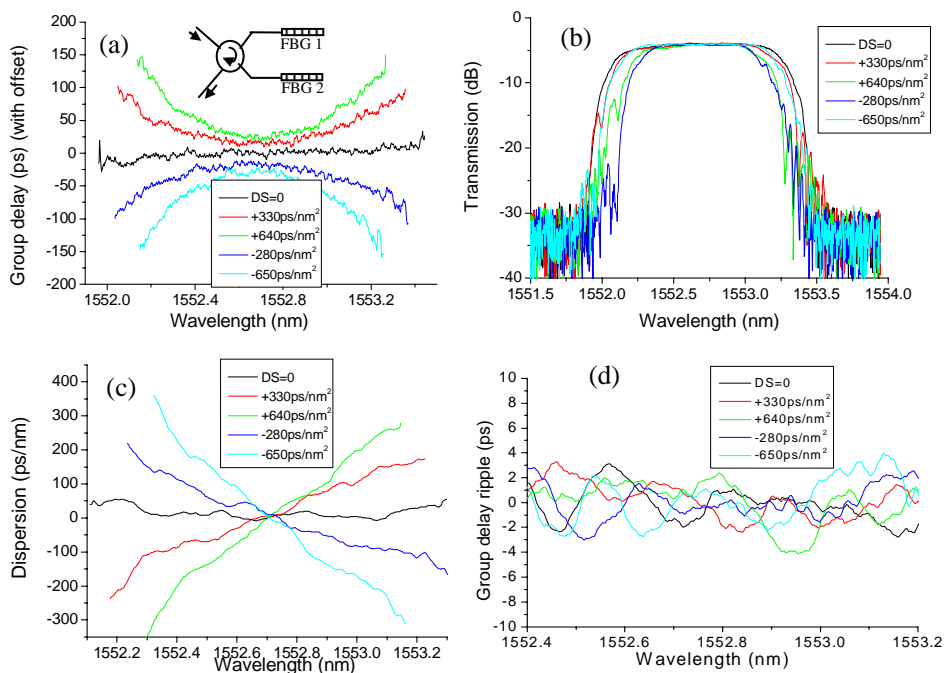


Fig. 6. Measured group delay (a), transmission spectra (b), dispersion (c) and group delay ripples (d) of a tunable dispersion slope compensator at different dispersion slope settings. Inset in (a) shows the schematic configuration of the TDSC.